Journal of Catalysis **199,** 123–131 (2001)
doi:10.1006/jcat.2000.3136, available online at http://www.idealibrary.com on IDEAL®

Anode Materials for Low-Temperature Fuel Cells: A Density Functional Theory Study

E. Christoffersen,*,† P. Liu,* A. Ruban,* H. L. Skriver,* and J. K. Nørskov*,[1]

*Center for Atomic-Scale Materials Physics, Department of Physics, and †Interdisciplinary Research Center for Catalysis (ICAT), Technical University of Denmark, DK-2800 Lyngby, Denmark

Received September 27, 2000; revised December 4, 2000; accepted December 4, 2000; published online March 9, 2001

Based on density functional calculations, we discuss the effect of alloying Pt with other metals for use as anode catalyst materials in low-temperature fuel cells. We discuss why a few parts per million of CO in the H_2 fuel can poison Pt surfaces and how this problem can be alleviated by alloying, and an extensive data base of the effect of alloying on the reactivity that includes all binary combinations of the transition metals to the right in the periodic table is given. We also discuss the effect of surface segregation and give a calculated data base of segregation energies of binary transition metal alloys. Based on extensive Monte Carlo simulations we show that while the adsorbate-free surface of a $Ru_{0.5}Pt_{0.5}$ alloy has no Ru in the first layer, the presence of CO can move some Ru to the surface, but all these Ru atoms are covered by CO. © 2001 Academic Press

Key Words: **fuel cells; anode materials; alloy catalysts; CO poisoning; Pt Ru alloy; DFT; Monte Carlo.**

1. INTRODUCTION

Fuel cells based on polymer proton conductors offer new hope for a stable, low-temperature energy source for, e.g., vehicles. Fuel cells function as electro-chemical engines that convert the chemical energy released in the reaction of H_2 and O_2 into electrical energy. The so-called proton exchange membrane fuel cells (PEMFCs) use a polymer membrane as the electrolyte. At the anode hydrogen is oxidized to protons and electrons,

$$H_2 \rightarrow 2H^+ + 2e^-.$$

The electronically insulating membrane allows the protons to move through it to the cathode where the oxygen is reduced:

$$O_2 + 4H^+ + 4e^- \rightarrow 2H_2O.$$

The presence of liquid water is a necessity for the membrane to function efficiently and this limits the temperature range in which it can be operated to 60–100°C (1). The H_2 used as fuel for the fuel cell is usually produced from natural gas or from methanol (MeOH) or other liquid fuels by stationary or on-board reformer systems. CO is a byproduct of such processes and it is very hard to avoid 10–100 ppm of CO in the feed gas. An alternative is the so-called direct methanol fuel cell (DMFC), which has the drawback of a less efficient and more complicated anode reaction, in addition to problems with MeOH crossover (2, 3).

The low temperature of operation puts strong limits on the purity of the fuel. As little as approximately 20 ppm of CO in the H_2 severely poisons a pure Pt catalyst surface (1). Various Pt-based alloys have been proposed to alleviate this problem, the current standard solution being a PtRu alloy catalyst, which is considerably more CO tolerant than the pure Pt catalyst (4). Watanabe and co-workers (5) have investigated the electrocatalytic oxidation of H_2 in the presence of CO on different Pt alloys using a rotating disk electrode setup and they found that in addition to PtRu the PtFe, PtNi, PtCo, and PtMo alloys show good CO resistance. The surfaces of these alloys were shown to consist of a thin layer of Pt with an electronic structure different from pure Pt. There are two possible ways in which alloying could change the CO sensitivity of H_2 oxidation (1). One is that, e.g., Ru promotes CO oxidation, thus removing CO from the surface (4, 6). This is consistent with the recent observation by Hayden and co-workers (7) that CO oxidation on Pt(110) is promoted by Ru in the surface region. The other possibility is that alloying decreases the CO stability more than the stability of H on the surface. This is consistent with the experiments of Behm and co-workers (8), who used thermal desorption to show that Pt overlayers on a Ru(0001) surface bonds CO considerably weaker than the clean Pt(111) surface.

In the present paper we focus on the question of the competitive CO and H_2 adsorption. On the basis of extensive "ab initio" density functional calculations we study the origin of CO poisoning of Pt surfaces and the effects of alloying on the CO poisoning. We initiate the discussion by introducing a simple model of the kinetics of proton formation at a metal surface in the presence of H_2 and CO in the

[1] To whom correspondence should be addressed. Fax: (+45) 45 93 23 99. E-mail: norskov@fysik.dtu.dk.

0021-9517/01 $35.00

gas phase. The main parameters controlling the effect of CO on the kinetics are the CO and H_2 adsorption energies, and we therefore continue by giving a short review of the effects that control the adsorption strength of CO and H_2 on transition metal surfaces. We show that a single surface parameter controls both adsorption energies, and discuss how to change the adsorption energies by alloying. In this connection we give an extensive data base of the effect of alloying on the reactivity by considering all binary combinations of the transition metal to the right in the periodic table.

If we want to affect the surface chemical properties by alloying, it is important to know the surface composition as a function of bulk composition. We therefore also present an extensive calculated data base of segregation energies for binary transition metal alloys and discuss how adsorption can affect surface segregation. We present Monte Carlo simulations for the Pt/Ru system in the presence of CO and show that under all reasonable conditions, the only free sites present on the surface are Pt atoms and all the effects on the surface chemistry are related to modifications of the Pt surface properties by subsurface Ru. Finally, we discuss which would be the best binary alloys for anode materials from the point of view of having the largest H/CO ratio on the surface of the catalyst.

2. THE KINETICS OF PROTON FORMATION

We start by giving a simple description of the kinetics of the production of protons at a metal surface. We do not intend for this to be a detailed treatment of the kinetics, but rather to illustrate qualitatively the effect of CO. We consider the three reactions

$$H_2 + 2* \rightleftharpoons 2H* \quad [1]$$

$$CO + * \rightleftharpoons CO* \quad [2]$$

$$H* \rightarrow H^+ + e^- + *, \quad [3]$$

where a $*$ denotes a free site on the surface. We assume that this is the rate limiting part of the kinetics. The rate of H^+ production is given by the forward rate of the last step (we assume that the backward rate is negligible),

$$r = k_3\theta_H \quad [4]$$

where k_3 is the forward rate constant of Eq. [3] and θ_H denotes the coverage of adsorbed H atoms on the surface. We do not include H_2O adsorption and dissociation or the possibility of electrochemical CO oxidation in the present treatment. Such effects could be included, but we choose at present to concentrate on the effects that do not include water.

We will assume that the first two steps are in quasi-equilibrium. This means that we can express the coverages of adsorbed CO and H in terms of the equilibrium constants K_H and K_{CO} for the two steps and the pressures P_{H_2} and P_{CO} of H_2 and CO as

$$\theta_H = \sqrt{K_H P_{H_2}}\,\theta_* \quad [5]$$

$$\theta_{CO} = K_{CO} P_{CO} \theta_*. \quad [6]$$

Using $\theta_{CO} + \theta_H + \theta_* = 1$ we can solve for θ_H, which in turn gives the total rate of proton production through Eq. [4],

$$\theta_H = \frac{\sqrt{K_H P_{H_2}}\,(1-\theta^0_{CO})}{1+\sqrt{K_H P_{H_2}}\,(1-\theta^0_{CO})}, \quad [7]$$

where

$$\theta^0_{CO} = \frac{K_{CO} P_{CO}}{1 + K_{CO} P_{CO}} \quad [8]$$

is the coverage of CO on the surface in the absence of any other molecules in the gas phase.

The equilibrium constants are given by expressions like

$$K_i = \exp(-(\Delta E_i - T\Delta S_i)/kT), \quad i = H, CO, \quad [9]$$

where ΔE_i and ΔS_i are the changes in energy (enthalpy) and entropy upon adsorption. Assuming the adsorbed species to have only high-frequency vibrational modes (on the scale of k_BT) $\Delta S_H = 136$ J mol^{-1} K^{-1} and $\Delta S_{CO} = 202$ J mol^{-1} K^{-1}. In the limit $\theta \ll 1$ Eq. [7] can be reduced to

$$\theta_H = \sqrt{K_H P_{H_2}}\,(1-\theta^0_{CO}) \approx \frac{\sqrt{P_{H_2}}}{P_{CO}} \exp\left(-\left(\frac{1}{2}\Delta E_H - \Delta E_{CO}\right)\Big/ k_B T\right), \quad [10]$$

showing that the performance is given mainly by the difference in the H and CO adsorption energy. This is a natural result since it is the competition between H and CO adsorption that determines θ_H.

The starting point for our discussion of anode materials is the close-packed Pt(111) surface. The values of ΔE_{H_2} and ΔE_{CO} have been measured and calculated for this surface in the gas phase. In an electrochemical cell the presence of the electrolyte and the cell voltage will affect these values (9). The present results are therefore most relevant for small overpotentials, but we expect the qualitative aspects to also be relevant to the electrochemical situation. Measurements of ΔE_{H_2} vary between 0.42 and 1.34 eV (10) and calculations give values between 0.5 and 0.8 eV, depending on the exchange correlation energy functional used (11). We will be using the most recent value of $\Delta E^0_{H_2} = 0.5$ eV in the following. Measured values of ΔE_{CO} vary between 1.39 (12)

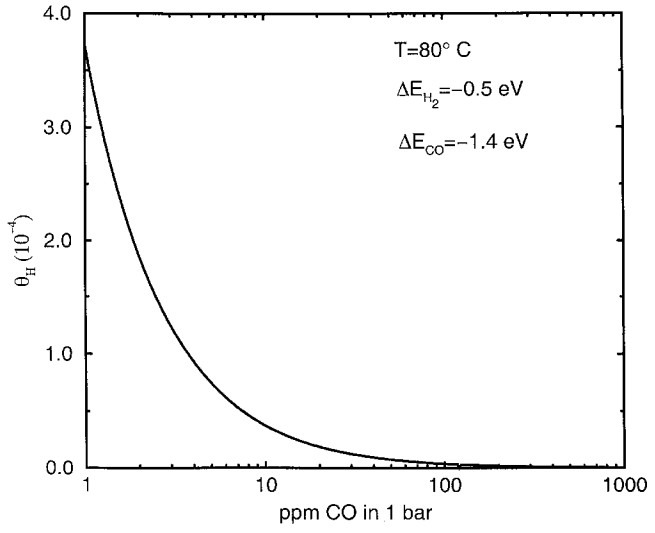

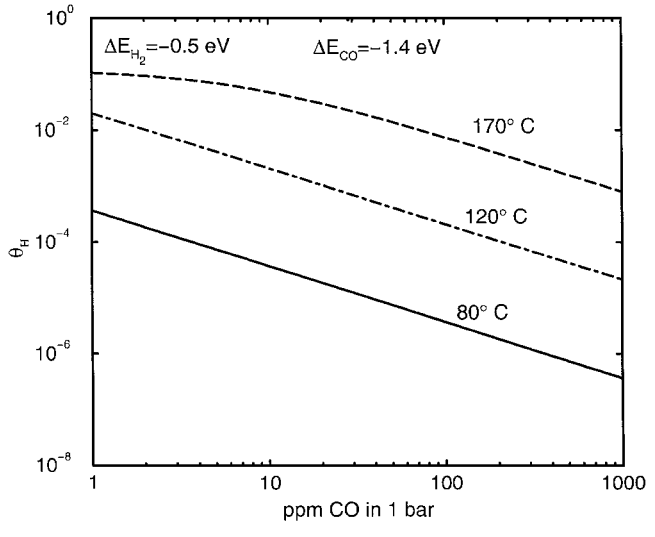

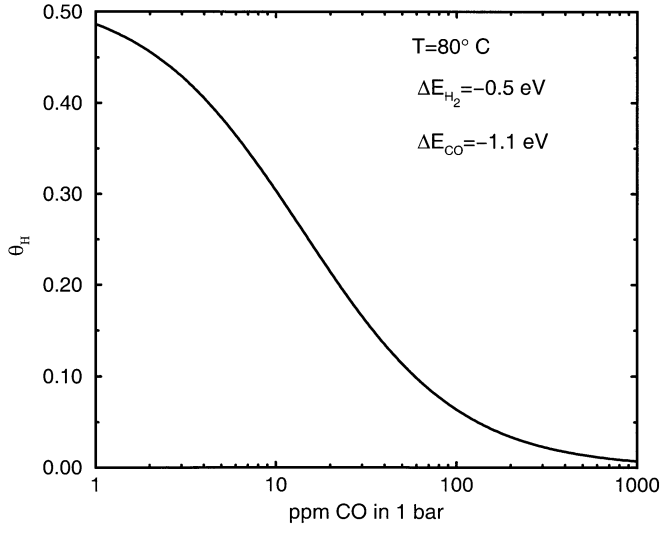

FIG. 1. Calculated variation in the hydrogen coverage θ_H according to Eq. [7] as a function of the CO partial pressure. The H_2 partial pressure is 1 atm.

and 1.94 eV (13), depending on the method used. Calculated values vary between 1.39 (14) and 1.82 eV (15), depending on the method used to treat exchange and correlation effects. The most accurate number seems to be around $\Delta E^0_{CO} = 1.4$ eV, and this is the value we will be using in the following.

If we use these parameters and ask the question what the hydrogen coverage (and thus the total rate from Eq. [4]) will be as a function of CO partial pressure, we get the result shown in Fig. 1. It is clearly seen that at 80°C the H coverage decreases strongly for CO concentrations above about 10 ppm. This is in accordance with the experimental observations of Pt-based fuel cell performances in the presence of CO (1), lending further support to the kinetics and the parameters used here. Increasing the temperature will clearly alleviate the problem considerably, so a proton conductor working at high temperatures or other cell types, such as the phosphoric acid fuel cells (PAFC) operating around 200°C (1), does not have this problem.

In order to see what kind of changes in the CO adsorption energy are needed to change the strong CO poisoning effect at 80°C, we consider now the effect of variations in ΔE_{CO}. We will see below that there is a tendency that ΔE_H varies along with ΔE_{CO} from one metal to the next, so we will make variations in both parameters in the vicinity of ΔE^0_H and ΔE^0_{CO} so that

$$\Delta E_H = \Delta E^0_H + \alpha\left(\Delta E_{CO} - \Delta E^0_{CO}\right). \qquad [11]$$

In Fig. 2 we show the hydrogen coverage as a function of the CO adsorption energy, ΔE_{CO}, for $\alpha = 1$. Two conclusions are immediately clear from the figure. First, it is clear

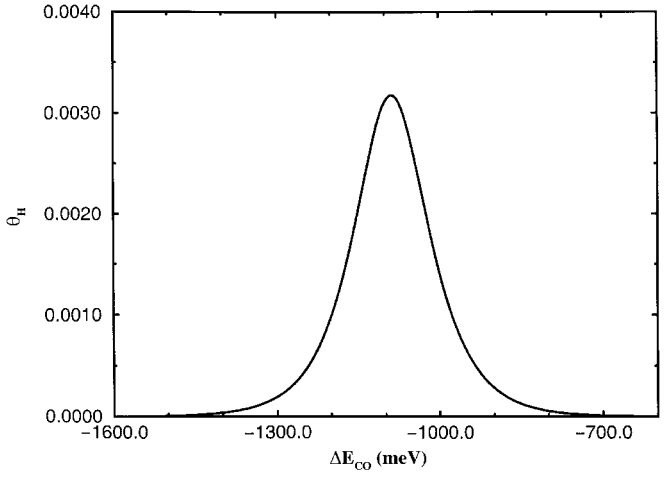

FIG. 2. Calculated variation in the hydrogen coverage θ_H according to Eq. [7] as a function of the binding energy of CO. The hydrogen binding energy is assumed to follow the variation in the CO binding energy according to Eq. [11] and $\alpha = 1$ has been used as the relative strength of the variations in the H_2 and CO bond energies. The partial pressure of H_2 is 1 atm and the CO concentration is 10 ppm.

that there is a strong dependence of the hydrogen coverage and thereby of the rate on the CO partial pressure. Secondly, the effect is strongly dependent on ΔE_{CO}. As ΔE_{CO} is increased (the strength of the CO–surface bond is decreased), the hydrogen coverage increases strongly. If the bond strength gets too small, on the other hand, the H coverage also becomes too small (for $\alpha \neq 0$), simply because ΔE_H and ΔE_{CO} follow each other according to Eq. [11]. These results indicate that there is an optimal window of CO (and H) bond strengths for the reaction to proceed.

3. ELECTRONIC FACTORS AFFECTING CO BONDING AND H_2 DISSOCIATION

The bonding of CO and H_2 to transition metal surfaces is extremely well studied, and a detailed understanding of the factors controlling the bond strength has been established. We will follow the description of Hammer and Nørskov (16). Figure 3 summarizes calculated CO adsorption energies on different 4*d* and 5*d* transition metals. The general trend is that the further to the left in the transition metal series, the stronger the adsorption.

In Fig. 3 the CO adsorption energy, ΔE_{CO}, is plotted as a function of a single parameter describing the electronic properties of the metal surface without any adsorbates, the *d*-band center ϵ_d. This parameter measures the energy of the metal *d* states relative to the Fermi energy, and it can be seen that the higher in energy the *d* states are, the stronger the interaction. It has been shown in detail how to understand this behavior in terms of the interaction between the CO molecular states and the metal electronic states (16). For the present purposes, we will simply accept the correlation between adsorption strength and ϵ_d. Since the *d* states move up in energy toward the left in the transition metal series as the *d* shell becomes less and less occupied, the interaction strength increases, but a similar effect can be obtained for a given metal as its surroundings are changed. Figure 3 includes results for CO on a Pt overlayer on Ru. In the latter case the Pt *d* states have been shifted down in energy and the CO–Pt interaction is reduced accordingly. This result clearly illustrates the possibilities in bimetallic systems for modifying the properties of a given metal.

The trends in the variation of hydrogen chemisorption energies are much the same as for CO (11). In Fig. 3 we include results for H chemisorption energies on different transition metals. Clearly, the constant α in Eq. [11] is close to 1.

3.1. *Trends in Reactivity for Bimetallic Surface Alloys*

Having established that both the hydrogen and the CO adsorption energies depend on the same surface parameter, ϵ_d, the question arises how this parameter can be varied. The question we ask is how the properties of a given metal can be changed by alloying it with another metal. For simplicity we will only consider cases where one of the components segregates to the surface so that there is no mixed phase in the first surface layer. Most of our conclusions are not affected by this choice, though, as we will show below. There are two key parameters of interest here: (i) how does the alloying or overlayer formation modify the electronic structure, and in particular ϵ_d, and (ii) will the metal that we are considering be present at the surface ? In the following we first consider point (i). The question of the surface concentration of the components in an alloy is the subject of the subsequent section.

In Fig. 4 we show calculated changes in ϵ_d for a number of late transition metals at the surface of all the others. For each metal considered we compare the ϵ_d to the values for the elemental metals, which are given in the diagonal of the matrix. This means that if the change in ϵ_d is negative (blue color), a single layer of the metal in question on top of another metal will tend to be less reactive (bind CO and H weaker according to the correlation described above) than the metal itself and vice versa.

Two major trends can be clearly seen in Fig. 4: a quite strong negative shift of the *d*-band center of 4*d* and 5*d* late transition metals on the surfaces of 3*d* metals and, vice versa, a substantial positive shift of the center of the *d* band of 3*d* metals on the surfaces of 4*d* and 5*d* metals. As explained in Ref. (21) this is mainly a size effect that is a consequence of the contraction or expansion of the lattice spacing of the pseudomorphic overlayer compared to the surface of pure metal. Another factor that governs the *d*-band shift of the overlayer is the number of *d* electrons of the underlying host metal: The smaller the number of the valence *d* electrons it has, the deeper the shift of the ϵ_d of the overlayer element. In fact, the effect is so strong for Pt and Pd on the surfaces of IIIb–Vb transition metals (Sc, Y, La, Ti, Zr, Hf, V, Nb, Ta) that the reactivity should be almost suppressed. Why it does not work in practice, however, is the metal–adsorbate interaction, which reverses the surface segregation behavior making the catalytic elements, like Pt and Pd, unaccessible at the surface.

4. SEGREGATION ENERGIES FOR TRANSITION METAL ALLOYS

Before we consider the complete picture, which includes interaction of the alloy components with an adsorbate, we will first have a look at the prediction of the theory in the case of clean surfaces of binary random alloys A_xB_{1-x}. The key parameter that can be used to estimate the surface composition at a given bulk composition and temperature is the surface segregation energy. Although it in general depends on the alloy composition, crystal structure, and surface orientation, the overall trends can be observed and understood on the basis of the segregation energies of impurities (i.e.,

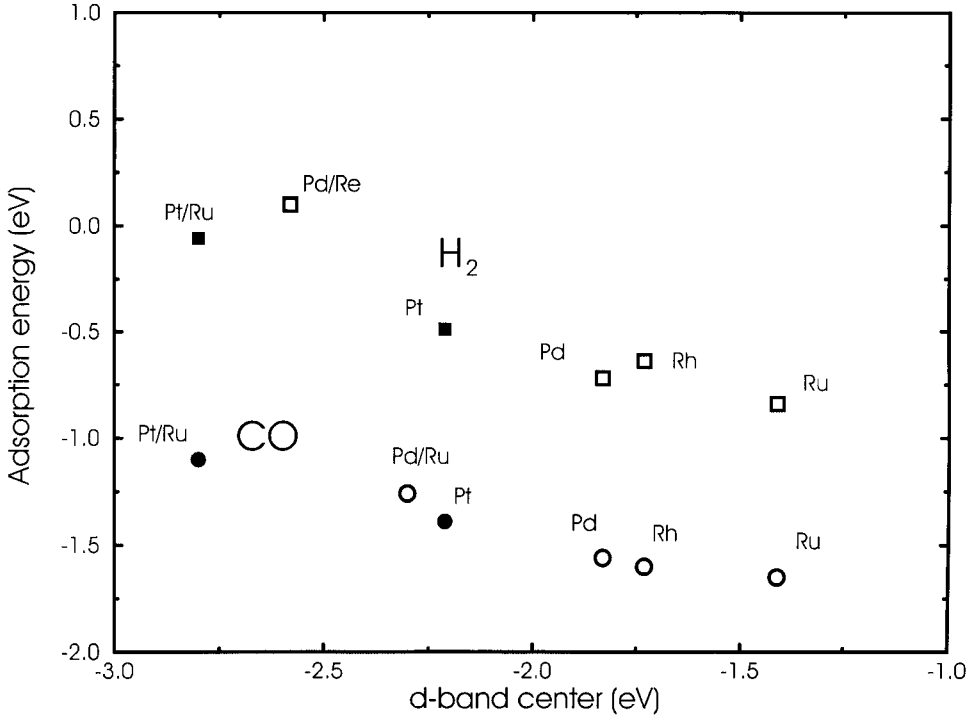

FIG. 3. Calculated variations in the CO (only atop) and H_2 chemisorption energies on 4*d* (open symbols) and 5*d* (filled symbols) transition metals shown as a function of the center of the *d* bands ϵ_d. The values of ϵ_d is taken from LMTO calculations, Fig. 4. The CO and H_2 adsorption energies on the pure 4*d* metals are taken from Ref. (17) except for CO on Ru (18) and CO on Rh (19) and are calculated using the RPBE functional. The results for Pt and Pt/Ru are new calculations. The adsorption energy for H_2 on Pd/Re is estimated from Ref. (20), where the PW91 functional has been used to calculate the difference between the pure Pd and a monolayer of Pd on Re. The adsorption energy of CO on Pd/Ru is estimated from Ref. (15), where the PW91 functional has been used to calculate the difference between the pure Pd and a monolayer of Pd on Ru. Details of the calculations can be found in these references.

dilute limit of binary alloys) in the otherwise pure hosts. In fact, in the case of the alloys of the late transition metals the composition dependence of the segregation energies is very small.

In Fig. 5 we show the results of ab initio calculations of the surface segregation energies of transition metal *impurities* at the most closed-packed surfaces of other transition metals as a color-coded matrix (22–24). Here, red colors correspond to negative segregation energies and, hence, to segregation of the impurity (solute) toward the surface of the host, and blue colors correspond to positive segregation energies and, hence, to the situation where the impurity prefers to remain in the interior of the host.

From Fig. 5 one can immediately see several trends in the surface segregation phenomena. First, every subblock of the matrix for different periods of the Periodic Table looks very similar. This is a consequence of the fact that, in general, the surface segregation energy is proportional to the difference of the surface energies of the alloy components, which in turn are proportional to the cohesive energies. The latter have a well-known parabolic behavior as a function of the number of valence *d* electrons in the metal. The metals at the beginning and at the end of each *d*-band series have the lowest cohesive and consequently the smallest surface energies, and this determines their segregation properties: they segregate toward the surfaces of the central transition metals, which are usually confined to the bulk region of the alloy.

There are, of course, some additional features in the surface segregation behavior, connected, for example, to structural and magnetic effects (for details see (22)). Several alloys of Pt with, e.g., Ni and Cu form ordered alloys, and this also means that mixed phases can be important at the surface. Nevertheless, the main conclusion that can be drawn from the results presented in the figure is that the late transition metals such as Pt and Pd have promising catalytical properties since they readily segregate toward the surface of other transition metals.

4.1. The Effect of Adsorption

The presence of an adsorbate can change the surface composition of an alloy significantly compared to the case where there is no gas present. In this case, and if there are no

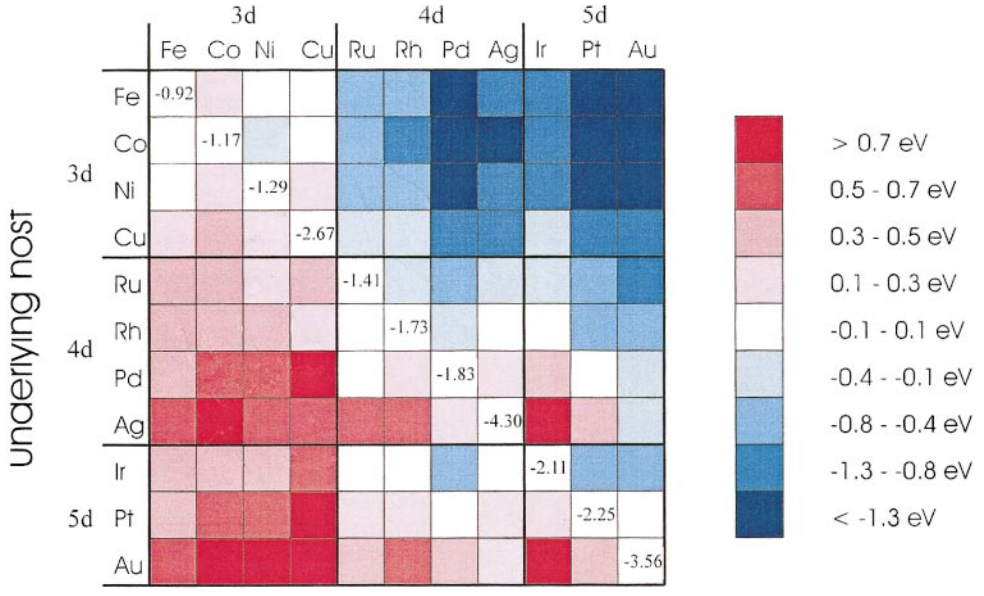

FIG. 4. Color-coded changes in the *d*-band centers for pseudo-morphic overlayers of transition metals on other transition metals. The calculations are based on fully self-consistent density functional calculations and are taken from Ref. (21).

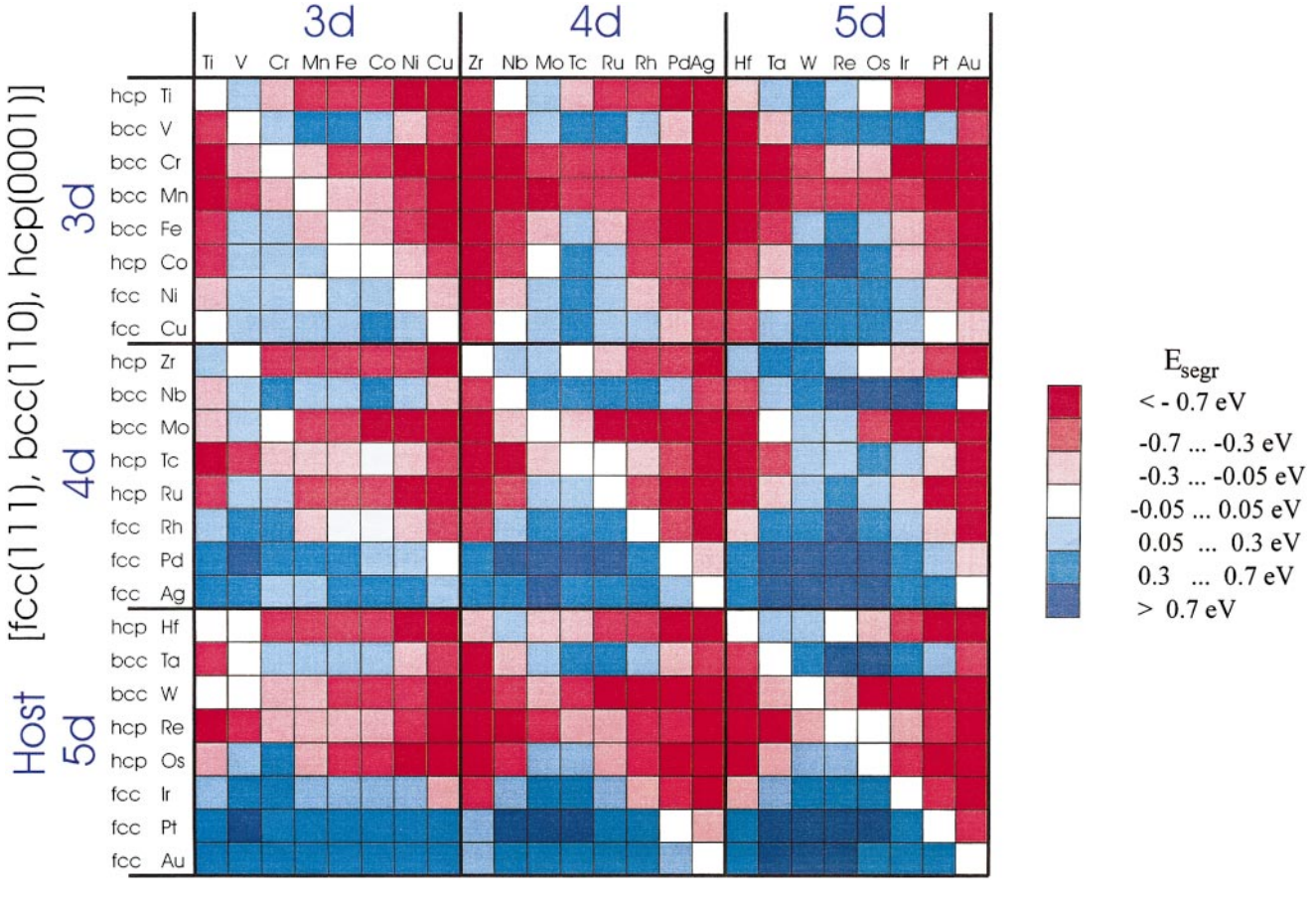

FIG. 5. Color-coded surface segregation energies of transition metal impurities (solute) for the closed-packed surfaces of transition metal hosts. The details of the calculations and the underlying database is to be found in Ref. (22).

kinetic limitations, the condition for element A to be at the surface can be formulated in terms of the surface segregation energy $E^A_{\text{segr}}(B)$ of element A in the A_xB_{1-x} alloy, and the binding energies of the adsorbate (adsorption energies) to the A and B atoms at the surface, $E^A_{\text{ads}}(B)$:

$$E^A_{\text{segr}} + E^A_{\text{ads}} - E^B_{\text{ads}} < 0. \quad [12]$$

The CO adsorption energies on the surface of *pure* elements grow fast and approximately linearly with *decreasing* number of d electrons, from late to earlier transition metals, cf. Fig. 3. This means that in the presence of CO there could be segregation reversal in the binary Pt or Pd alloys with earlier transition metals, caused by strong interaction of CO with atoms of the earlier transition metal, which pulls them out to the surface. Although, for a rough estimate, one can use the adsorption energies of gases on the surfaces of pure metals, it is worth remembering that the real values of $E^{A(B)}_{\text{ads}}$ in the alloy can be strongly modified due to interaction between the alloy components as described in the previous section; i.e., the late transition metal becomes less reactive with adsorbate in the presence of the earlier transition metal and vice versa. In the following we will discuss the problem of adsorbate-induced segregation in more detail.

4.1.1. Simulation technique. In order to study the phenomenon of adsorbate-induced segregation we have developed a Monte Carlo method, which treats both the segregation and the adsorption/desorption at the surface.

In our simulations we include adsorption and desorption from/to a gas phase, surface diffusion of the adsorbate, and diffusion from the bulk to the surface and back in the alloy. The alloy is treated as a host material with some impurity atoms present, the adsorbate layer consists of adsorbate atoms/molecules and free sites, and the gas phase is described by the pressure of the adsorbing atom or molecule. A typical size of our unit cell is 100×100 atoms with 9 alloy layers, and we impose periodic boundary conditions in the two directions parallel to the surface.

For simplicity we only allow for on-top adsorption. This is a good starting point for CO adsorption, because CO tends to adsorb on top of the late transition metals (13, 25–27), which we have chosen to study. We represent the energy of the system as a sum over the nearest-neighbor pair potentials, V_{ij},

$$E = \frac{1}{2}\sum_{R,R'} V_{ij}, \quad [13]$$

where i and j stand for impurity, host, adsorbate, or free site, depending on the type of atoms in the nearest-neighbor R and R' sites.

The interaction between two adsorbates is set to be repulsive ($V_{\text{ads,ads}} = 0.5$ eV), such that the maximum coverage will be $\theta = 0.33$. This is done for simplicity and should not change the conclusions. The adsorption energies discussed above are used for the interaction between metal and adsorbate ($V_{\text{host/imp,ads}}$). The interaction between a free site and another site is set to 0; that is, $V_{\text{host,free}} = V_{\text{imp,free}} = V_{\text{ads,free}} = V_{\text{free,free}} = 0$. This way the driving force for the segregation will be the lack of interaction at the surface.

The interaction between the metal atoms is derived from the segregation and mixing energies in the following way. The segregation energy can be defined as the energy gain by interchanging an impurity atom in the bulk with a host atom in the surface in the dilute limit. This leads to

$$E_{\text{segr}} = (Z - Z_s)(V_{\text{host,host}} - V_{\text{host,imp}}), \quad [14]$$

where Z is the coordination number for a bulk atom, and Z_s is the coordination number for a surface atom.

The mixing energy is a measure of the tendency of the impurity to form a random surface alloy instead of islands on the surface and is defined as

$$E_{\text{mix}} = \frac{\partial^2 E_{\text{surf}}(x_s, x_b)}{\partial x_s^2}, \quad [15]$$

where $E_{\text{surf}}(x_s, x_b)$ is the surface energy and x_s and x_b are the impurity concentrations in the surface and the bulk, respectively. Assuming a random alloy and letting $x_b \to 0$ (28) we get

$$E_{\text{mix}} = Z_1 2((V_{\text{imp,imp}} - V_{\text{host,imp}}) + (V_{\text{host,host}} - V_{\text{host,imp}})), \quad [16]$$

where Z_1 is the number of bonds in the surface plane. These two Eqs. [14] and [16] are sufficient to determine the three remaining parameters ($V_{\text{host,host}}$, $V_{\text{imp,imp}}$, and $V_{\text{host,imp}}$) because it is the energy differences ($V_{\text{host,host}} - V_{\text{host,imp}}$) and ($V_{\text{imp,imp}} - V_{\text{host,imp}}$) that govern the segregation. This has been thoroughly tested. So in general we set $V_{\text{host,host}} = 0$ and then determine $V_{\text{imp,imp}}$ and $V_{\text{host,imp}}$ from Eqs. [14] and [16].

5. THE PtRu SYSTEM

In order to test the effect of CO adsorption on surface segregation, we have investigated a $Pt_{50}Ru_{50}$ alloy under different conditions. This also allows us to investigate in detail if Ru at the surface of a PtRu alloy is important for the improved properties of the alloy as anode catalyst from the point of view of the H/CO coverage. We use the calculated values of $E_{\text{segr}} = 0.59$ eV and $E_{\text{mix}} = 0.11$ eV obtained by the methods discussed above (24).

Our conditions were $T = 353$ K and $P_{\text{CO}} = 10$–100 ppm of 1 bar. In order to estimate the CO adsorption energy on Ru on a $Pt_{50}Ru_{50}$ alloy we have calculated the d-band shift of a surface Ru impurity in $Pt/Pt_{50}Ru_{50}(111)$ using the Green's function method described in Ref. (24). The calculated d-band shift is 0.09 eV. The CO adsorption energy

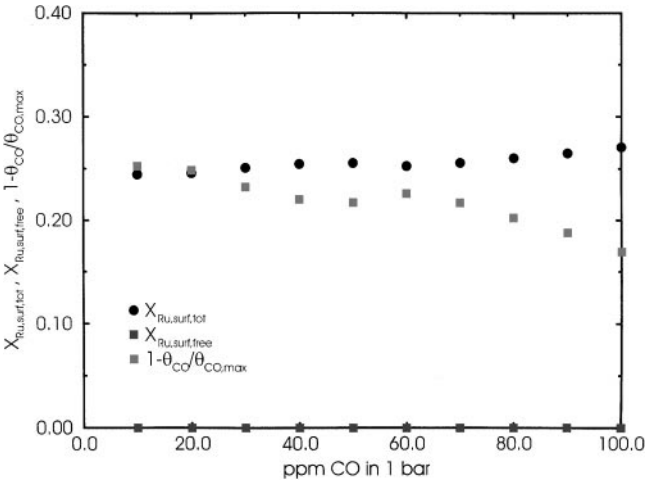

FIG. 6. The total mole fraction of Ru in the surface, the mole fraction of free Ru in the surface, and the amount of free surface sites as a function of CO content in the gas at 80°C.

varies approximately as −0.5 times the *d* band shift (cf. Fig. 3), and the adsorption energy should therefore be approximately 0.04 eV larger (stronger) on Ru on the alloy than on clean Ru(0001). This leads to an estimate of the CO adsorption energy of 1.69 eV. For CO on Pt atoms on the alloy surface we have calculated the adsorption energy for CO on Pt/Ru(0001) to be 1.10 eV using the method of (17).

When these parameters are used in the Monte Carlo simulations we get some segregation of Ru to the surface, but all the Ru sites at the surface are covered by CO, cf. Fig. 6. The Pt sites on the other hand are quite free from CO.

We conclude from these simulations that the superior performance of PtRu compared to pure Pt as an anode catalyst can, at least in part, be attributed to a modification of the CO/Pt adsorption energy due to the presence of Ru in the bulk.

We note in this context that according to our DFT calculations Ru modifies the adsorption of CO on Pt in the surface for Pt impurities in Ru (cf. Fig. 4), when Pt is in the surface of a $Pt_{50}Ru_{50}$ alloy (cf. the discussion above), and when CO is adsorbed on Pt at the surface of a Pt(111) crystal with Ru, which has segregated to the second layer.

6. CHOOSING GOOD CANDIDATES FOR ANODE MATERIALS

We are now in a position to discuss in some detail why some alloys may be more suited than others as anode material. As discussed above a good material must bind CO weaker than pure Pt, but not too weakly, since that implies that also H is bound too weakly, cf. Fig. 3. In this connection it must also be remembered that if the surface becomes too unreactive, H_2 dissociation may become highly activated, and this may in itself limit the rate (11). In addition, the metal in question must segregate to the surface under reaction conditions. Finally, none of the metals involved must form stable oxides, since alloys involving these metals will tend to segregate an oxide phase during exposure to oxygen or water.

Exchanging Pt for a completely different metal is difficult. Pd is the most obvious possibility, but even Pd binds CO stronger than Pt (cf. Fig. 3). All the transition metals to the left of Pd or Pt bind CO stronger, not weaker, than Pt and Pd. Ag and Au, on the other hand, do not bind H_2 at all (11), and on Cu H_2 adsorption is activated and thermo-neutral (11). The possibility is therefore to make Pt (or Pd) slightly less reactive, or to make some of the other metals much less reactive. We will concentrate on the former possibility in the following.

Of the combinations of metals considered in Fig. 4, Pt should become less reactive at the surface of all the metals considered here except Ag and Au, and these are also the only metals where Pt should not segregate to the surface. Alloys with Ir, Rh, Ru, Cu, Ni, Co, and Fe should therefore produce less reactive Pt and thus a better anode catalyst. Most of these systems have been identified experimentally to work in this way (1, 5). In particular, our findings are in excellent agreement with results from Watanabe and coworkers (5), who found that the surfaces of Pt alloys consisted of a thin layer of Pt with an electronic structure different to that of pure Pt and they concluded that this different electronic structure of Pt was responsible for the lowering of the equilibrium concentration of CO on the surface. Pt forms ordered alloys with the 3*d* metals Cu, Ni, Co, and Fe, and at the surface of these metals there may therefore be appreciable amounts of other metals compared to that of Pt (29–31). This can dilute the positive effect of alloying, but should not change it completely (32).

7. SUMMARY

We have presented a comprehensive picture of the factors determining the reactivity of alloy surfaces, and have shown that these considerations can be used to understand why some binary alloys of Pt are better anode materials than pure Pt. We have concentrated on effects not including water. The CO oxidation by dissociated water is important at high overpotentials and must be included in a complete treatment, but we have chosen to single out the effect of the competition of CO and H_2 for surface sites. The main conclusions are that adding another metal to Pt changes the position of the *d*-band center for Pt, and the position of the *d*-band center is a measure of the adsorption energy of an adsorbate. It is, however, important to take adsorbate induced segregation into account as in certain cases it can make the Pt unaccessible at the surface. The increased CO tolerance of the PtRu alloy compared to that of pure Pt can be explained by this electronic effect, which lowers the CO

adsorption energy on Pt and thereby gives more free Pt in the surface. We note that a weaker CO–Pt bond also makes the CO more reactive in connection with CO oxidation at higher overpotentials.

ACKNOWLEDGMENTS

The present work was in part financed by the Danish Research Councils through Grant 9501775 and by ICAT sponsored by the Danish Research Council through the "Chemistry Programme." The Center for Atomic-Scale Materials Physics is sponsored by the Danish National Research Foundation.

REFERENCES

1. Hoogers, G., and Thompsett, D., *Catttech* **6**, 106 (2000).
2. Liu, L., Viswanathan, R., Fan, Q., Liu, R., and Smotkin, E. S., *Elec. Acta* **43**, 3657 (1998).
3. Hogarth, M. P., and Hards, G. A., *Platinum Metals Rev.* **40**, 150 (1996).
4. Gasteiger, H. A., Marković, N., Ross, P. N., and Cairns, E. J., *J. Phys. Chem*. **98**, 617 (1994).
5. Watanabe, M., Igarashi, H., and Fujino, T., *Electrochemistry* **67**, 1194 (1999).
6. Oetjen, H. F., Schmidt, V. M., Stimming, U., and Trila, F., *J. Electrochem. Soc.* **143**, 3838 (1996).
7. Davies, J. C., Hayden, B. E., and Pegg, D. J., *Elec. Acta* **44**, 1181 (1998).
8. de Mongenot, F. Buatier, Scherer, M., Gleich, B., Kopatzki, E., and Behm, R. J., *Surf. Sci.* **411**, 249 (1998).
9. Koper, M. T. M., van Santen, R. A., Wasileski, S. A., and Weaver, M. J., *J. Chem. Phys.* **113**, 4392 (2000).
10. Somorjai, G. A., "Introduction to Surface Chemistry and Catalysis," Wiley, New York, 1994.
11. Hammer, B., and Nørskov, J. K., *Nature* **376**, 238 (1995).
12. Seebauer, E. G., Kong, A. C. F., and Schmidt, L. D., *Surf. Sci.* **176**, 134 (1986).
13. Brown, W. A., Kose, R., and King, D. A., *Chem. Rev.* **98**, 797 (1998).
14. Watwe, R. M., Cortright, R. D., Nørskov, J. K., and Dumesic, J. A., *J. Phys. Chem. B* **104**, 2299 (2000).
15. Hammer, B., Morikawa, Y., and Nørskov, J. K., *Phys. Rev. Lett.* **76**, 2141 (1996).
16. Hammer, B., and Nørskov, J. K., *in* "Chemisorption and Reactivity on Supported Clusters and Thin Films" (R. M. Lambert and G. Pacchioni, Eds.), pp. 285–351, Kluwer Academic, Dordrecht, The Netherlands, 1997. B. Hammer and J. K. Nørskov, *Adv. Catal.* **45**, 71 (2000).
17. Hammer, B., Hansen, L., and Nørskov, J. K., *Phys. Rev. B* **59**, 7413 (1999).
18. Bollinger, M., private communications.
19. Mavrikakis, M., and Nørskov, J. K., private communications.
20. Pallassana, V., Neurock, M., Hansen, L. B., Hammer, B., and Nørskov, J. K., *Phys. Rev. B* **60**, 6146 (1999).
21. Ruban, A., *et al*., *J. Mol. Catal. A* **115**, 421 (1997).
22. Ruban, A. V., Skriver, H. L., and Nørskov, J. K., *Phys. Rev. B* **59**, 15,990 (1999).
23. Christensen, A., Ruban, A. V., Stoltze, P., Jacobsen, K. W., Skriver, H. L., and Nørskov, J. K., *Phys. Rev. B* **56**, 5822 (1997).
24. Ruban, A. V., and Skriver, H. L., *Compt. Mater. Sci.* **15**, 119 (1999).
25. Koestner, R. J., Hove, M. A., and Somorjai, G. A., *Surf. Sci.* **107**, 439 (1981).
26. Hollins, P., and Pritchard, J., *Surf. Sci.* **89**, 486 (1979).
27. Pfnür, H., Feulner, P., and Menzel, D., *J. Chem. Phys.* **79**, 4613 (1983).
28. This limit is used, because the segregation energies have only been calculated in this dilute limit.
29. Rodriguez, J. A., and Goodman, D. W., *Science* **257**, 897 (1992).
30. Bertolini, J. C., Tardy, B., Abon, M., Billy, J., Delichère, P., and Massardier, J., *Surf. Sci.* **135**, 117 (1983).
31. Castro, G. R., Schneider, U., Busse, H., Janssens, T., and Wandelt, K., *Surf. Sci.* **269/270**, 321 (1991); Linke, R., Schneider, U., Busse,H., Becker, C., Schröder,U., Castro, G. R., and Wandelt, K., *Surf. Sci.* **307–309**, 407 (1994); Becker, C., Schröder, U., Castro, G. R., Schneider, U., Busse, H., Linke, R., and Wandelt, K., *Surf. Sci.* **307–309**, 412 (1994).
32. Nieuwenhuys, B. E., *Surf. Rev. Lett.* **3**, 1869 (1996).